Heliyon 9 (2023) e20934

Contents lists available at ScienceDirect

Heliyon

journal homepage: www.cell.com/heliyon

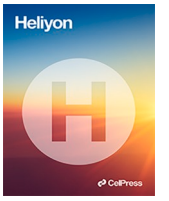

Laser speckle reduction using polymer-stabilized liquid crystals doped with Ag nanowires

Xin Jiang [a], Weilong Zhou [a], Wei Wang [a], Zichun Le [a,*], Wen Dong [b]

[a] College of Science, Zhejiang University of Technology, Hangzhou 310023, PR China
[b] College of Environment, Zhejiang University of Technology, Hangzhou 310023, PR China

ARTICLE INFO

Keywords:
Laser speckle reduction
Liquid crystal devices
Polymer-stabilized liquid crystals
Ag nanowires
Degree of scattering
Response time

ABSTRACT

Miniaturized and pure static devices are expected to be used in laser-imaging systems for speckle reduction. In this study, a pure static device based on polymer-stabilized liquid crystal (PSLC) doped with Ag nanowires was developed to effectively suppress laser speckles. The concentrations of the polymer and Ag nanowires in the PSLC were optimized, and then the PSLC devices were fabricated. A measurement system was set up to characterize the electro-optical properties of the fabricated PSLC devices. Subsequently, a laser projection system was built to demonstrate the speckle-reduction performance. Moreover, the degree of scattering and response time of the developed PSLC devices were investigated and discussed. A PSLC doped with 0.02 wt% Ag nanowires and 3 wt% polymer having a device size of $2 \times 2 \times 0.1$ cm^3 was demonstrated to produce a speckle-reduction efficiency of 51.4 % under very low driving voltages. The experimental results verified effectiveness and superiority of the developed speckle reduction method based on PSLC doped with Ag nanowires.

1. Introduction

With the development of laser technology, laser sources have been widely used in projection displays [1–3]. This is because of the advantages of lasers with high brightness, wide color gamut, low energy consumption, long lifetime, and small size [4]. However, the high coherence of the laser beam leads to different optical path differences when it irradiates rough surfaces, which causes interference of the scattered light waves in space and in turn generates bright and dark granular spots, called speckles [5]. Speckles significantly reduce the imaging quality of the laser projection and even cause vertigo to the viewer. Therefore, speckle reduction has been extensively studied.

Speckle reduction can be done in two main ways, either by reducing the spatial and temporal coherence of laser beams or by generating uncorrelated independent speckle patterns for time averaging within the resolution time of the human eye or camera. Wavelength, angular, and polarization diversity are mainly used in the former, specifically using random lasers, multimode fibers, light pipes, arrays of optical waveguides, diffusers, and diffraction optical elements (DOEs). The latter usually requires the introduction of mechanical devices for further speckle reduction [6–19]. The simplest and most effective speckle-reduction method is the introduction of a moving diffuser, which generates angular diversity through light scattering and achieves time-averaging of intensities through diffuser movement [9–12]. In our previous studies, we proposed a flexible DOE with reciprocating motion, which could reduce the speckle contrast to 4 % [15–17]. However, the introduced mechanical devices reduce the stability of the optical system and are not

* Corresponding author
E-mail address: lzc@zjut.edu.cn (Z. Le).

https://doi.org/10.1016/j.heliyon.2023.e20934
Received 29 June 2023; Received in revised form 11 October 2023; Accepted 11 October 2023
Available online 13 October 2023

conducive to miniaturization of laser projectors. Therefore, a static device based on the dynamic speckle-reduction method is warranted.

Liquid crystals (LCs) have been widely used in the display field because of their excellent electro-optical properties and have become ideal fillers for static diffusers. Some research groups have reported studies on speckle reduction by LCs [20–32] because LC molecules have unique birefringence properties and can be modulated by an electric field. LCs are typically used for speckle reduction in the form of polymer LC composites, in which dynamic transition between the scattering and transparent states can be achieved by voltage control. The scattering state is caused by the refractive index mismatch between the LC molecules and polymer. The scattering state is dynamically adjustable; therefore, the LC device can be considered as a moving diffuser. Liquid crystal polymer systems can be classified into polymer-dispersed liquid crystals (PDLC) and polymer-stabilized liquid crystals (PSLC) based on the polymer concentration. The PDLC scheme is the most commonly used scheme for speckle reduction based on LCs [20–23]. Recently, a PDLC device with specially designed interdigitated electrodes was proposed for speckle reduction [20], and the speckle reduction performance was improved by increasing the diversity of the electric field caused by the designed interdigitated electrodes. Eventually, the speckle contrast was reduced from an initial value of $C_0 = 0.71$ to $C = 0.32$ under a driving voltage of 150 V. A reduction efficiency of 55 %, defined as $(1 - C/C_0)$, was achieved. Similarly, another scheme of doping SiO_2 particles in LCs was proposed, which eventually achieved a speckle-reduction efficiency of 40 % under a driving voltage of 180 V [21]. Owing to the high polymer content of PDLC, a relatively high external voltage is usually required to drive the LC molecules. Therefore, the PDLC-based method has disadvantages of slow response, high power consumption, and a complicated fabrication process. In contrast, PSLC contain lower polymer concentrations, which can achieve the desired deflection of LC molecules at low voltages [24–26]. For instance, a speckle-reducing efficiency of 83 % was observed by the addition of a redox dopant to a chiral nematic LC, which can effectively increase the density of current carriers and enhance the electrohydrodynamic instability (EHDI) [24]. However, the speckle-reduction system was very complicated and was composed of an LC device and two additional optical devices, including two glass diffusers and a light tube, which led to a larger light intensity loss, higher power consumption, and larger optical system size. Moreover, the higher speckle-reduction efficiency was caused by the combined effect of the LC, diffusers, and light tubes [24]. A speckle-reduction efficiency of approximately 54.7 % was reported using PSLC with 5 wt% polymer inside the wedge cell [25]; however, it required a very complex fabrication of wedge cells.

Hereafter, we briefly clarify the dynamic scattering mechanism in the polymer LC devices, which plays a key role for reducing the spatial or temporal coherence of the lasers [31,32], and in turn causes the speckle suppression. For a polymer LC device, the scattering degree correlates with the spatial decoherence capability, while the response time determines the temporal decoherence capability. When a polymer LC device is placed in the laser imaging systems as a speckle-suppression device, the speckle contrast can be written as [5].

$$C = \frac{\sqrt{\sum_{n=1}^{N} \bar{I}_n^2}}{\sum_{n=1}^{N} \bar{I}_n} \tag{1}$$

where N is the number of decorrelated speckle patterns, n is positive integer and $\bar{I}$ is the average intensity. Assuming that all of the speckle patterns have the same average intensity, then the speckle contrast (C) can be reduced by $\frac{1}{\sqrt{N}}$. Therefore, by adjusting the alignment of LC molecules within the polymer LC devices, it becomes possible to effectively disrupt the coherence of incident light waves, resulting in a reduction in speckle size and intensity. Subsequently, the time decoherence capability is further improved by increasing the response speed of the LC devices to increase N during the integration time.

Although devices based on LCs have been used to reduce speckles, few studies have reported on their mechanism, especially the effect of the response time and scattering degree of LC devices on the performance of speckle reduction. Most studies focused on the material, polymer concentration, driving voltage, frequency, and cell shape, which did not directly affect speckle contrast [20–26]. There have been some discussions on the degree of scattering [20,25]; however, the dynamic process has not been accurately described. The response time, which is an important factor in dynamic speckle reduction, has rarely been mentioned in previous studies.

In this study, a novel LC device was proposed and investigated in a laser projection system to develop a miniature pure static device with adjustable dynamic scattering for better speckle suppression, faster response, and easier fabrication. This device is based on PSLC doped with Ag nanowires, since Ag nanowires have lower resistance and higher conductivity [30], which is beneficial to drive the liquid crystal molecules and maintain the uniformity of the electric field. It thus can obviously improve the dielectric response of the PSLC. First, a PSLC mixture for scattering was developed, and the concentrations of the polymer and Ag nanowires in the mixture were optimized. We then fabricated PSLCs doped with Ag nanowires and measured their electro-optical properties related with the performance of speckle suppression. Subsequently, a laser projection system was set up to demonstrate the performance of the developed PSLC devices and the proposed speckle-reduction method. The laser speckles are suppressed by superimposing more uncorrelated independent speckle patterns during a certain integration time. Uncorrelated independent speckle patterns are stimulated by the degree of scattering, and a shorter response time corresponds to more speckle patterns being involved in the superposition process. The effect of the response time and scattering degree of LC devices on the performance of speckle reduction has been carefully investigated for the first time. Finally, with a low voltage of 6 V and high voltage of 50 V, the speckle contrast decreased from the initial value of $C_0 = 0.321$ to $C = 0.156$ and the speckle-reduction efficiency was 51.4 %. The experimental results verified that the PSLC doped with Ag nanowires was superior to conventional polymer liquid crystal devices.

2. A novel PSLC device for speckle reduction

The schematic structure and working principle of a PSLC device are shown in Fig. 1. The device is composed of an optically transparent box made of ITO glass with a thin polyimides layer on the inside surface for the vertical alignment of LC molecules and the filling material of the box, which is a mixture of different components of polymer and negative LC molecules.

When driving voltage is not applied, the negative LC molecules are aligned perpendicular to the ITO glass by the action of the orientation layer and polymer network (Fig. 1(a)). This is the transparent state with an extremely high transmittance. When a driving voltage is applied, the negative LC molecules tend to get aligned parallel to the ITO glass by the electric field force (Fig. 1(b)). However, because of the restriction of the polymer network, LC molecules get randomly oriented macroscopically. This corresponds to the scattering state with a low transmittance. In this study, Ag nanowires were doped into the above-mentioned mixture for the filling material to form a novel PSLC device for laser speckle reduction. Fig. 1(c) and (d) show the transparent and scattering states of the developed PSLC device, respectively. The transparent state of the developed PSLC device corresponds to the "off" state. When the voltage is applied to the PSLC, the dynamic scattering occurs, making it non-transparent, which corresponds to the "on" state.

2.1. Materials

The LC mixtures used in the developed PSLC device included a negative LC mixture HNG 30400-200 and polymer (RM82) from HECHENG DISPLAY (China), and a photo-initiator (Irg651) from ALADDIN, China. The negative LC mixture HNG 30400-200 has the following parameters: clear point temperature $T_{NI} = 94$ °C, dielectric anisotropy $\Delta\varepsilon = -8.3$, and refractive index difference $\Delta n = 0.149$. The molecular structures of RM82 and Irg651 are shown in Fig. 2. The LC mixture was doped with Ag nanowires (XFNANO, China) with a diameter of 30 nm and length of 20 mm. An LC hollow cell (NLC-08VA) was custom-made by The North LCD Engineering R&D Center, China. The cell was very small, with a size of $2 \times 2 \times 0.1$ cm^3 and a light window of 1×1 cm^2. The distance between the two ITO glasses was 8 μm, with the vertically aligned layer on both internal surfaces.

2.2. Fabrication of PSLC devices

Fig. 3 illustrates the fabrication process of the PSLC devices. These were fabricated using photopolymerization. The LC mixture containing HNG30400-200, RM82, and Irg651 was stirred using a thermomixer (JXH-100, TUOHE, China) for 2 h at 60 °C. The Ag nanowire LC mixture was manufactured using the following procedures [30]. First, ethanol-dispersed Ag nanowires were prepared by mixing Ag nanowires (10 mg) with 1 mL ethanol and then sonicating it for 30 min at room temperature. Next, the LC mixture and ethanol-dispersed Ag nanowires were transferred into a centrifuge tube and sonicated for 30 min at 60 °C. Finally, ethanol was completely removed from the PSLC mixture, and it was kept at room temperature for 24 h. Note that the prepared mixture should be protected from light to avoid precuring effects.

The LC hollow cell was produced using two ITO electrodes with the vertical alignment layer on both internal surfaces and separated

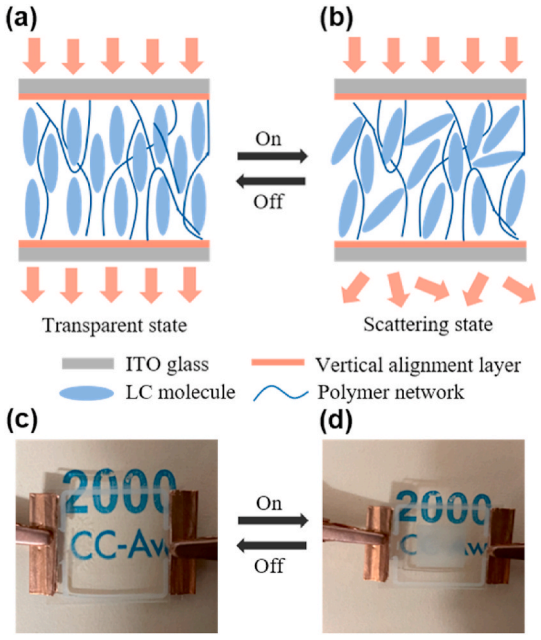

Fig. 1. Schematic diagram of a PSLC (a) without (Transparent state) and (b) with a driving voltage (Scattering state), and the photo of the developed PSLC sample (c) without ("off" state) and (d) with a driving voltage ("on" state).

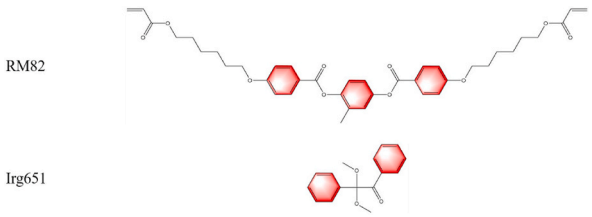

Fig. 2. Molecular structures of the polymer and photo-initiator.

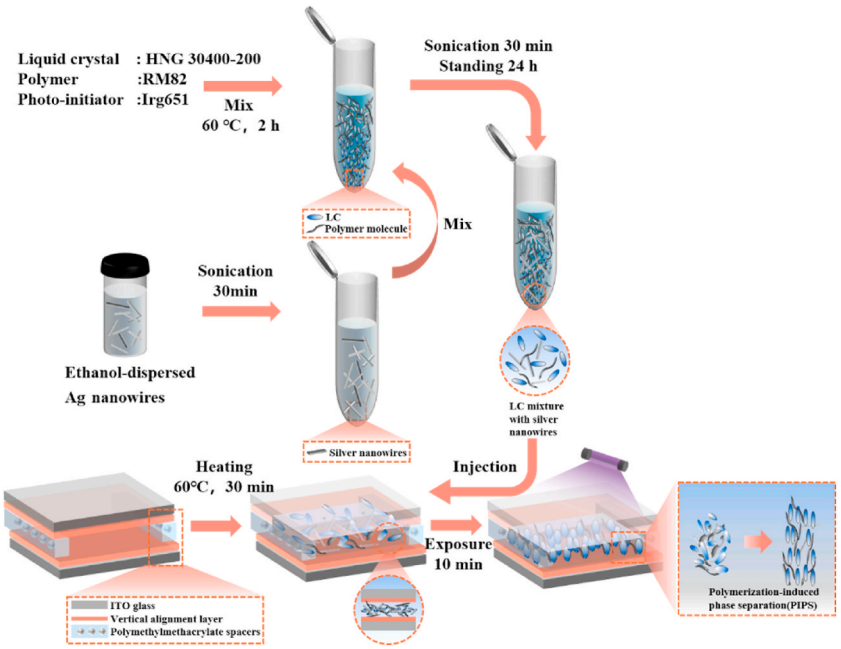

Fig. 3. Schematic diagram of the manufacturing process of a PSLC device.

by an 8 μm polymethylmethacrylate (PMMA) spacer. Before filling the prepared mixture into the cell, it was mixed at room temperature for 1 h. At the same time, the cell was placed on a hot plate at 60 °C for 20 min. Next, the mixture was filled into the LC hollow cell via capillary action in the isotropic phase. The filled LC cell was then kept on a hot plate at 60 °C for 30 min to homogenize the mixture. Finally, it was sealed using UV-curable glue (NOA65) and exposed to UV light with a wavelength of 365 nm for 10 min at 5 mW/cm^2 to achieve polymerization-induced phase separation (PIPS).

To investigate the effect of the concentrations of polymer RM82 and Ag nanowires on the speckle-reduction performance of the developed PSLC devices, a number of PSLC samples, which had polymer concentration of 3–7 wt% with an increment of 1 wt% and the Ag nanowires concentration from 0.01 to 0.1 wt% with an increment of 0.01 wt% were fabricated. Higher polymer concentrations were found to require much higher driving voltages. On the contrary, the influence caused by the Ag nanowires concentration was weak. Therefore, the optimal concentrations of polymer and Ag nanowires were determined, and four PSLC samples were chosen for further experiments. The parameters of the four chosen samples are shown in Table 1; the compositions of the samples include the concentrations of polymer contents ranging from 3 to 5 wt% (samples A1-A3) and the concentrations of Ag nanowires at 0.02 wt% (sample B1).

Table 1
Composition of samples A1–A3 and B1.

	Composition [wt%]			
Sample	RM82	Silver nanowires	HNG30400-200	Irg651
A1	3	0	96.80	0.20
A2	4	0	95.80	0.20
A3	5	0	94.80	0.20
B1	3	0.02	96.78	0.20

3. Experimental setups and characterization

3.1. Characterization of electro-optical properties

The electro-optical properties of PSLC devices describe the response of a PSLC to an applied external electric field. Moreover, because the PSLC devices are used in a laser-imaging system for speckle reduction in this study, the electro-optical property related to the performance of speckle reduction was investigated. Therefore, we define and clarify all the parameters related to the characterization of PSLC devices. The maximum transmittance (T_{max}) of a PSLC device is the transmittance without driving voltage. The minimum transmittance (T_{min}) is the lowest transmittance value in the test voltage range. To measure the real transmittance value during the speckle-reduction procedure, the exposure time of the spectrometer was set to 40 ms (sensing time of human eyes) to measure the transmittance of the PSLC devices powered by an AC voltage at 25 Hz. Threshold (V_{th}) and saturation (V_{sat}) voltages refer to the voltages at which 10 % (T_{10}) and 90 % (T_{90}), respectively, of the overall change in transmittance occur. The response time includes the turn-on (t_{on}) and turn-off (t_{off}) response times; t_{on} is the time taken to switch from the transparent to scattering state (from T_{min} to T_{90}) with a certain AC voltage and t_{off} is that from the scattering to transparent state (from T_{max} to T_{10}) without any electronic power.

Fig. 4 schematically shows the experimental setup for the characterization of the electro-optical properties of the PSLC device, including the response time, transmittance, and voltage-transmittance (V-T) curves. The experimental setup includes an optical system, power system, and data processing system. A 520 nm laser diode (LP520P50, Thorlabs) was used as the light source for coherent illumination. A beam expander was used for beam expansion and collimation to make the laser beam more parallel and uniform. And a 4 mm diameter iris was used to control the beam size for adapting with the following photodetector. The collimated laser beam passes through the fabricated PSLC devices and illuminates a photodetector with a time resolution of 18 ns (DET20-20 M, GLGYZN, China). The power system consists of a function generator, voltage amplifier, and oscilloscope. The function generator (DG811, RIGOL, China) outputs an AC electric signal, which is amplified using a voltage amplifier (ATA-2031, Aigtek, China). Both the output electric signal from the function generator and the photodetector signal from the fabricated PSLC device were measured using an oscilloscope to compare and determine the response time. Moreover, a spectrometer (FLA4000, Flight, China) was used to measure the transmittance of the PSLC devices at different voltages.

3.2. Measurement of speckle contrast

The developed PSLC devices were applied in a laser-imaging system for laser speckle reduction. The optical system is shown in Fig. 5 and includes a laser diode with a beam expander, a developed PSLC device, and an imaging screen. The light source and power system were the same as those shown in Fig. 4. Here, iris is a variable diaphragm with an aperture of D_0, which is used to limit the beam size exactly to the light window of PSLC devices as well as to isolate the stray light. L1 and L2 are two lenses for the collimation of the laser beam, and L3 is the projection lens. The collimated laser beam passes the PSLC device and is imaged on the screen using a projection lens. A CMOS camera (DCC3260 M, Thorlabs) was used to capture the speckle images. The camera has 1936 × 1216 pixels with a pixel size of 5.86 × 5.86 μm^2. Additionally, S_1, S_2, S_3, S_4, S_5, S_6, and S_7 are the distances between the laser and iris, iris and L1, L1 and L2, L2 and PSLC device, PSLC device and L3, L3 and screen, and screen and CMOS camera, respectively. L1 has an aperture of $D_1 =$ 50.8 mm and focal length of $F_1 = 60$ mm; L2 has an aperture of $D_2 = 50.8$ mm and focal length of $F_2 = 100$ mm; and L3 has an aperture of $D_3 = 50.8$ mm and focal length $F_3 = 60$ mm. In our experiments, $S_1 = 50$ mm, $S_2 = 150$ mm, $S_3 = 160$ mm, $S_4 = 50$ mm, $S_5 = 60$ mm, $S_6 = 280$ mm, and $S_7 = 300$ mm, and the aperture of the iris was set to $D_0 = 6$ mm. Then, the image with speckle patterns was projected onto the screen and recorded by a CMOS camera with a focal length of 30 mm and F-number of 16. The exposure time of the CMOS

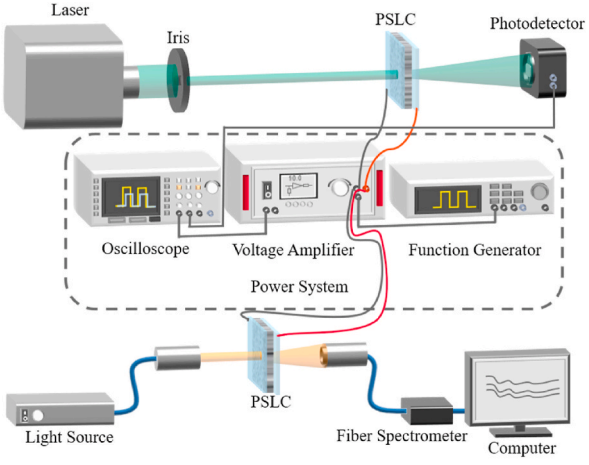

Fig. 4. Schematic illustration of the experimental setup to measure the electro-optical properties of PSLC devices at different applied voltages.

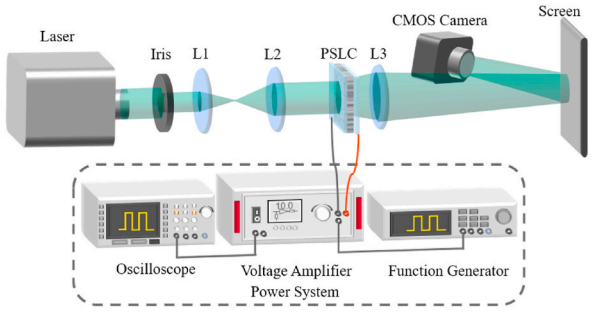

Fig. 5. Optical Scheme of the experimental laser-imaging system.v.

camera was set to 40 ms, which was matched with the sensing time of the human eye as well as the TV frame rate.

3.3. Characterization of PSLC

Firstly, a scanning electron microscopy (SEM) was used to characterize the polymer network structure of PSLC. To improve observation of the microstructure of polymer network within PSLC, PSLC was divided into two glass substrates containing polymer and liquid crystals. Then one of glass substrates was soaked in acetone for 48 h to remove liquid crystal molecules. After the immersion process, the PSLC sample was dried in a vacuum drying oven at 40 °C for 6 h to remove the residual acetone solution. Finally, the PSLC sample surface was analyzed by SEM (Gemini 500, Zeiss, Germany) after ion sputtering a 20 nm thick platinum film to improve conductivity.

Fig. 6 presents the measured results of polymer morphologies of samples A1-A3, which have different polymer concentrations, and sample B1, which is doped with Ag nanowires. As shown in Fig. 6(a), the sample with 3 wt% polymer concentration exhibited a sparse polymer network structure and a larger network width. Comparison of Fig. 6(a)–(c) reveals that an increase in polymer concentration resulted in a tighter polymer network structure and a decrease in the width of the network structure. This implies that higher concentrations of polymers can form stronger network structures, which will impose a stronger restriction on the arrangement of LC molecules when the driving voltage is applied.

However, it is notable that even with stronger restriction, LC molecules fast returned to a uniform orientation when the voltage was removed. In addition, the polymer network structure with doped Ag nanowires was comparable to that of undoped Ag nanowires when comparing B1 (Fig. 6(d)) to A1 (Fig. 6(a)). It has been found that doping 0.02 wt% Ag nanowires mainly improves the dielectric response speed of PSLC.

To ascertain the voltage-driven phase transition and scattering states of LCs, we observed scattering polarograms at varying

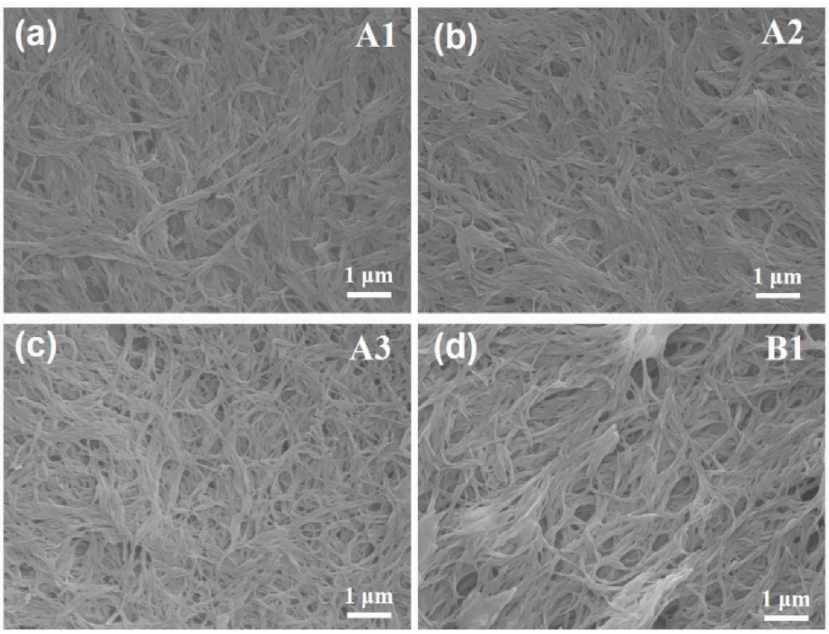

Fig. 6. SEM images of samples A1-A3 and B1. Magnification: 10 K. Exposure power: 10 KV. (a) A1, (b) A2, (c) A3, (d) B1.

voltages by polarization mode using a large depth-of-field 3D microscope (DSX1000, Olympus, Japan). Fig. 7 presents the corresponding POM images of the scattering states of PSLC that comprises different polymer concentrations at different voltages. Without an electric field or before reaching the threshold voltage, the LC molecules remained same direction due to the anchoring by the vertically oriented layers and polymer network of PSLC samples. As a result, their POM image maintained a black field. As an increase of the applied voltage, the LC molecules were deflected by the electric field, resulting in irregular perturbations of the LC molecules. The perturbations of the LC molecules changed the light phase, and in turn resulted in a scattering effect, which was reflected in the POM images with granular patterns. The scattering effect typically intensified with increasing electric field strength, leading to the observation of more granular patterns in the POM images. Comparison of Fig. 7(a)–(d) reveals that lower polymer concentrations in PSLC samples enable them to reach a scattering state more easily due to a less constricting polymer network structure corresponding to greater spatial decoherence. As the increase of polymer concentration, the voltage required to reach the same scattering state was higher. And the difference of scattering states among PSLC samples are largely determined by the density and strength of the polymer network structure, which is consistent with the SEM results.

4. Results and discussions

Dynamic scattering of PSLC devices is an important basis for reducing laser speckle, therefore the scattering degree of PSLC devices is the most important factor to be investigated in this study. Scattering degree is defined as the degree of spatial decoherence of the speckle patterns, which describes the random intensity fluctuations within the integration time. It is one of the most important factors that directly affect speckle reduction. Because the scattering caused by PSLC devices is dynamic, the scattering degree within the integration time can be characterized by the average transmittance and range of transmittance variation. The response time is defined as the time required for the PSLC device to transition between the transparent and scattering states at a periodic voltage. This reflects the number of speckle patterns that can be superimposed during the integration time to some extent. To the best of our knowledge, the response time, which is another important factor that reflects the temporal decoherence of speckle patterns and directly affects speckle reduction, has not yet been discussed in any study of speckle reduction by LC devices. Hereafter, the effects of the scattering degree and response time of the PSLC devices will be thoroughly investigated and discussed to clarify their relationship with speckle reduction.

4.1. Effect of the PSLC scattering degree on speckle reduction

To investigate the influence of speckle pattern variation of a PSLC device when different driving voltages are applied and identify the optimal modulation voltages, the PSLC devices were fabricated with different polymer concentrations (Table 1) and were used in the experimental setups shown in Section 3.

The speckle pattern variation is caused by the refractive index mismatch between the LC and the polymer network inside the PSLC devices, which can be modulated by dynamic voltage. Therefore, the average value of the transmittance ($\overline{T}$) and the range of transmittance variation (ΔT) at different modulation voltages can be measured separately at the same integration time to characterize the average scattering degree and modulation depth of the PSLC devices. Parameters $\overline{T}$ and ΔT were measured using the experimental setup shown in Fig. 4. A fiber spectrometer was used to probe the average transmittance. Before the measurements, the fiber

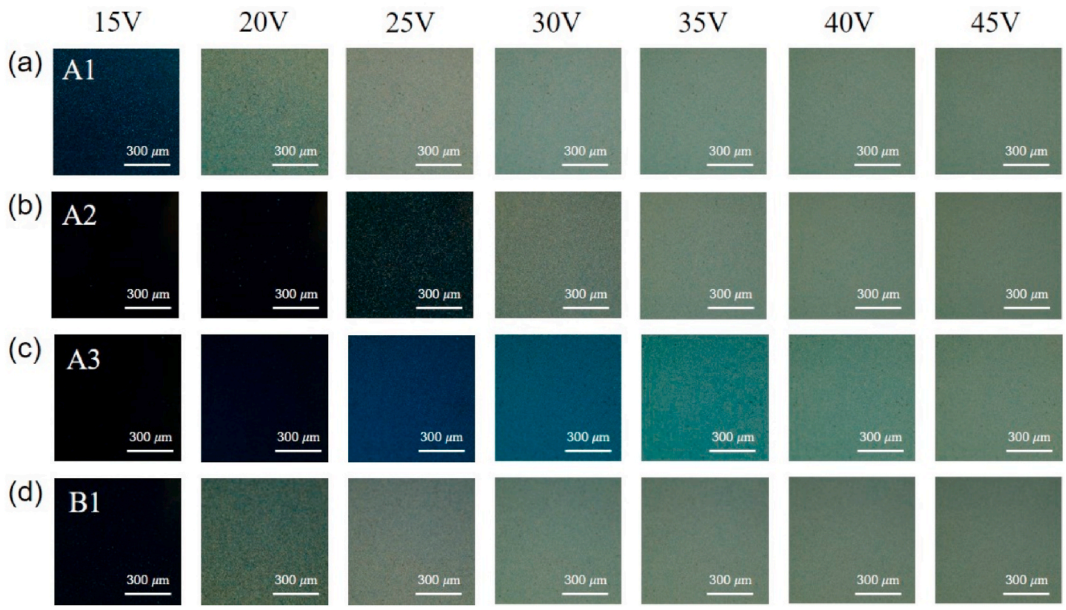

Fig. 7. Polarized images of samples A1-A3 and B1 under different electric field conditions: (a) A1, (b) A2, (c) A3, (d) B1.

spectrometer was calibrated to ensure that the initial transmittance was 100 %, and the scan time was set to 40 ms which is the same as the CMOS exposure time. Then, after the developed PSLC device was inserted in the light path, the intensity into the fiber spectrometer reduced owing to the scattering state of the PSLC device driven by a certain modulation voltage. However, because the fiber spectrometer has limited time resolution and cannot respond to transmittance variation over time, ΔT was measured using a photodetector. First, the maximum electrical signal without the PSLC device was measured and calibrated to the maximum transmittance value of the fiber spectrometer. Then, the maximum and minimum electrical signals were measured by applying a driving voltage to the inserted PSLC device, and the measured electrical signals were converted into the maximum and minimum transmittances (T_{max} and T_{min}). Consequently, the transmittance variation range can be expressed as $\Delta T = T_{max} - T_{min}$. The power system generated a square-wave signal for the PSLC device. The driving electric signal alternately changed between high voltage (V_h) and low voltage (V_l), and the driving frequency was set to 25 Hz. First, the optimal modulation voltages were experimentally determined when the low voltage was set to 0 V and the high voltage was varied from 0 to 50 V with increment of 2 V. Speckle contrasts were then measured using the experimental setup shown in Fig. 5. We set $V_h = V_l = 0$ for the "off" state of PSLC devices, and the speckle contrast measured under this condition is defined as the initial speckle contrast (C_0). The average transmittance ($\overline{T}$) of PSLC at various high voltages (V_h) is shown in Fig. 8(a). $\overline{T}$ of all three samples (A1–A3) decrease as V_h increased. When the applied driving voltage exceeds the threshold voltage V_{th}, the LC molecules begin to rotate in the direction of the electric field. The decrease in $\overline{T}$ was caused by a mismatch in the local refractive index, which resulted in dynamic scattering. Owing to the large rotation angle of the LC molecules, the scattering degree continues to dramatically increase with the increase in V_h, which in turn causes a continuous decrease in $\overline{T}$ during the integration time. However, the rotation angle of LC molecules is limited because of the anchoring effect of the polymer network. As a result, $\overline{T}$ varied slowly and eventually reached saturation. Fig. 8(a) shows that the average transmittance ($\overline{T}$) decreased with decreasing polymer concentration when the driving voltage was kept the same. A lower concentration of polymer forms looser or thinner polymer wires, and the weaker anchoring effect on LC results in a lower average transmittance.

When an AC electric field is applied to the PSLC devices, LC molecules will be switched from vertical to random alignment, which

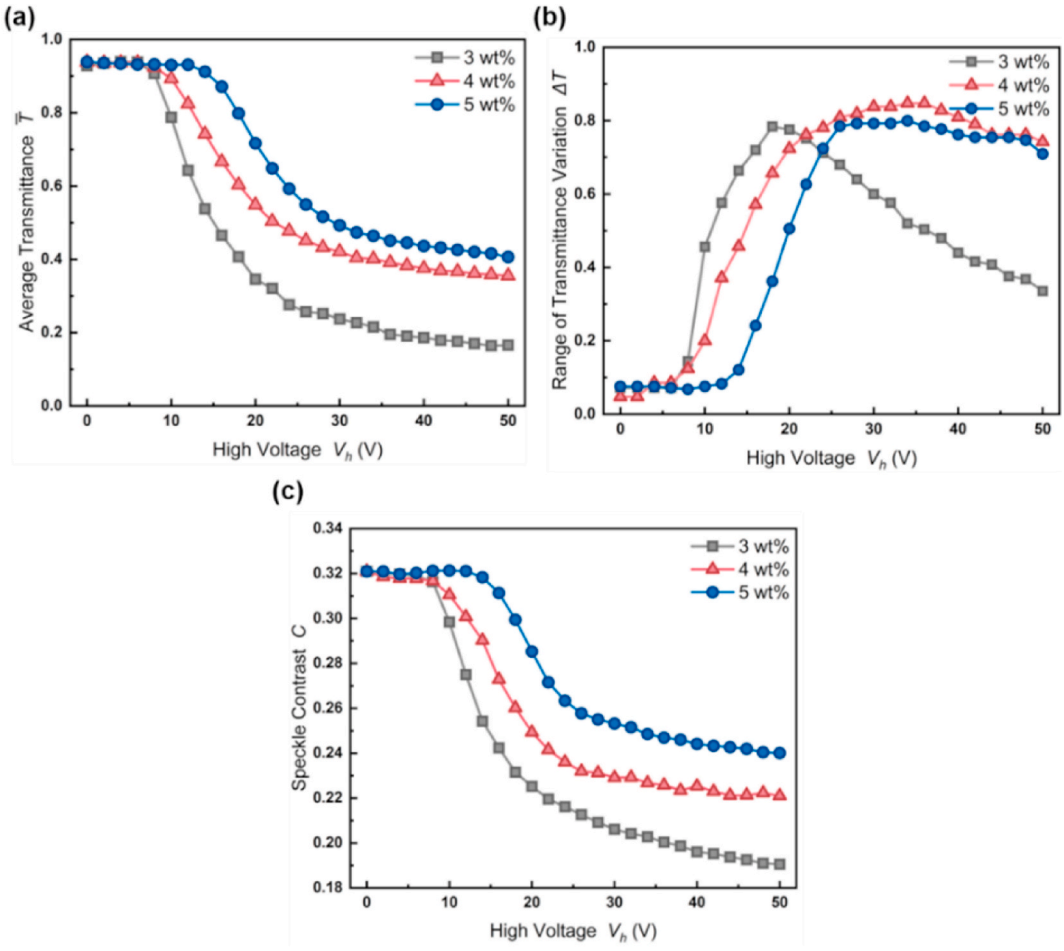

Fig. 8. Measured results for (a) high voltage–average transmittance (V_h–$\overline{T}$) curves, (b) high voltage-range of transmittance (V_h–ΔT) curves, and (c) dependence of the speckle contrast of PSLC devices with different polymer concentration on the variable high voltage.

cannot be reflected by $\overline{T}$. Instead, the range of transmittance variation ΔT can characterize the variation of scattering degree with variable high voltage. Thus, to realistically describe the variation process of PSLC devices under an AC electric field the variation of ΔT with V_h, which corresponds to the modulation depth of the LC molecules is plotted in Fig. 8(b). When a high voltage is applied, the PSLC devices maintain a low transmittance, which is dependent on the relationship between the electric field force and anchoring strength. The stronger the anchoring strength, the higher the driving voltage required, which in turn, corresponds to a higher degree of scattering, implying a higher degree of decoherence. When the high voltage is removed, the PSLC devices maintain high transmittance, which is dependent on the anchoring strength of the polymer network. The stronger the anchoring strength, the faster the LC molecules return to their initial state, resulting in a lower degree of scattering, which implies a lower degree of decoherence. As shown in Fig. 8 (b), ΔT for all the three samples increased sharply as the driving voltage increased toward saturation. After the saturation voltage V_{sat} was reached, ΔT for samples A2 and A3 became saturated and stabilized. In this state, the LC molecules have achieved maximum reorientation. For samples A2 and A3, the strong anchoring effect of the polymer network effectively restricted the rotation of the LC molecules. Therefore, the LC molecules did not undergo further rotations, which involved in overcoming the polymer network structure. This saturation behavior of ΔT can be attributed to the reached balance between the driving force of the applied electric field and the anchoring strength of polymer network. The stable arrangement of LC molecules and the limited anchoring effect imposed by polymer network prevented any significant changes in ΔT. However, ΔT for sample A1 showed a decreasing trend after reaching the maximum value. This phenomenon can be explained by the fact that the anchoring effect of the polymer network at 3 wt% was much weaker. The weaker anchoring effect results in a decreased constraint on the LC molecules by the polymer network. Consequently, when the alternating electric field with an oversaturation voltage is applied, the LC molecules are driven to overcome the constraints of the polymer network and then undergo significant rotation or flipping, which will disrupt the stability of the molecular orientation and increase the directional differences among the LC molecules. Simultaneously, the polymer network may undergo deformation, which will make the LC molecules unable to be fully restored to a uniform distribution after the removal of applied voltage. Consequently, a sustained decrease in ΔT was observed in the experiments. And the higher the voltage, the more pronounced this phenomenon. Because sample A1, under the supersaturated voltage, continues to maintain a high scattering state with dynamic modulation, the average transmittance of sample A1 was found to be much lower than that of samples A2 and A3, as shown in Fig. 8(a). Additionally, the corresponding voltage values when ΔT reached the threshold and saturation states were almost the same as those when $\overline{T}$ reached the threshold and saturation states, respectively. Both V_{th} and V_{sat} increased with an increase in anchoring strength. Thus, by changing the polymer concentration, we can adjust the electro-optical properties of PSLC devices, including the average transmittance, range of transmittance variation, and threshold and saturation voltages.

The speckle contrast (C) for all the three PSLC samples decreased as the driving voltage increased, as shown in Fig. 8(c). The variation tendency of C is similar to that of $\overline{T}$. A lower $\overline{T}$ indicates that the superimposed speckle pattern has better decoherence within the integration time. Therefore, C can be suppressed more effectively. When $\overline{T}$ of sample A1 reached saturation, C maintained a consistent decreasing trend. This phenomenon proves that the decrease in C is not simply caused by the larger dynamic deflection range of the LC molecules. As mentioned above, a lower transmittance implies a better decoherence effect and in turn a better speckle suppression. As the oversaturation state is concerned, due to $T_{\min}$ reaches a saturation state and remains constant, a lower $T_{\max}$ corresponds to a better decoherence effect. Therefore, in the case of sample A1 at the oversaturation state, the decrease in ΔT further promotes the reduction of speckle. After V_{sat} was reached, $\overline{T}$ and ΔT of samples A2 and A3 became saturated, leading to the saturation of the speckle contrast. Therefore, to optimize the speckle suppression effect, dynamic modulation at a greater deflection angle of the LC is required, which equates to a smaller $\overline{T}$ and relatively narrow ΔT. In addition, it is worth mentioning that ΔT is not smaller is better, a relatively narrow ΔT is expected for keeping in the dynamic modulation.

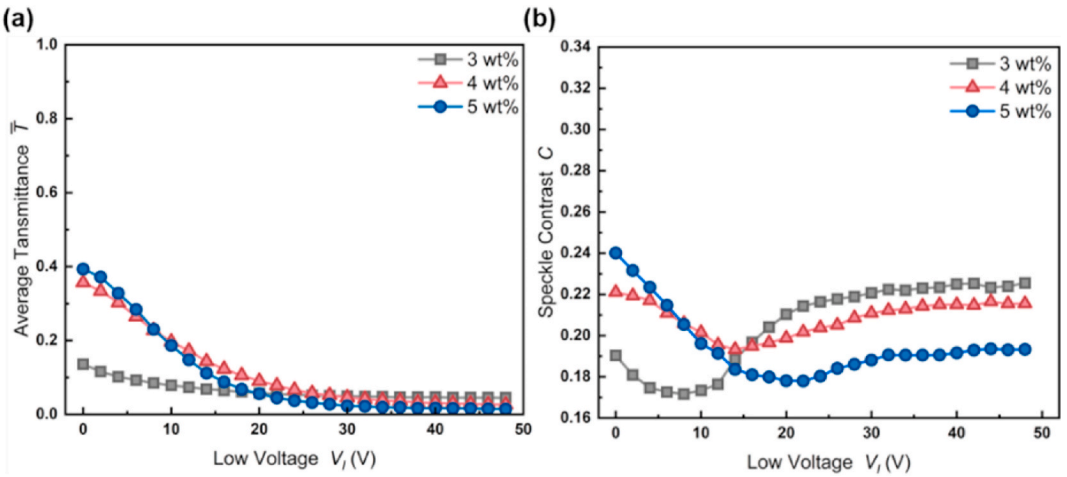

Fig. 9. Measured results for (a) low voltage–average transmittance ($V_l - \overline{T}$) curves and (b) dependence of the speckle contrast of PSLC devices with different polymer concentration on the variable low voltage.

Generally, a PSLC device with a lower polymer concentration exhibits better performance in speckle reduction. When V_h was set to 50 V, sample A1 with a 3 wt% polymer concentration achieved the most effective speckle reduction, for which the speckle contrast was reduced from 0.32 to 0.19 and the speckle-reduction efficiency was 40.6 %. Therefore, the optimized value of $V_h = 50$ V was used in subsequent experiments.

According to the above results, $\overline{T}$ and ΔT can be further adjusted by varying V_l to achieve more effective speckle reduction. Thus, V_h was set to 50 V, and V_l was increased from 0 to 48 V with increments of 2 V; the average transmittance was measured. Fig. 9 (a) shows the relationship between $\overline{T}$ and V_l, wherein $\overline{T}$ decreases as V_l increases because the deflection range of LC molecules gradually decreases and tends to be stable. At this point, the PSLC devices can be considered as a static modulation, which has an effect similar to that of a stationary diffuser. The difference in $\overline{T}$ at saturation was caused by the difference in the polymer concentration. The higher the polymer concentration, the greater the scattering degree. Thus, the final $\overline{T}$ values from low to high corresponded to polymer concentrations of 5, 4 and 3 wt%, respectively. When ΔT decreased to 0 as V_l increased, the parameter of ΔT was not of significance; therefore, the change in ΔT with V_l was not investigated.

The relationship between speckle contrast C and low voltage V_l is shown in Fig. 9(b). The minimum value of C appeared when V_l was near the threshold voltage V_{th} for all PSLC devices. When $V_l > V_{th}$, the speckle-reduction efficiency decreases and tends to become saturated. This phenomenon can be explained by the variation in the LC molecules' pointing vectors under different driving voltages. An LC molecule's pointing vector changes with the varying driving voltage from the microscopic point of view, which is mainly manifested in the change in its deflection angle and its variation range. When $V_l = V_{th}$, the LC molecules can be driven by high voltage. At this time, their deflection angle is large, exhibiting a perfect range of variation. Therefore, this state corresponds to a lower $\overline{T}$, implying a greater degree of decoherence. However, as V_l continues to increase, the range of deflection angle variation becomes smaller, leading to a decrease in the superimposition of speckle patterns within the integration time, which in turn leads to saturation of C. When C is in the saturated state, its variation with V_l is similar to that of $\overline{T}$ and the PSLC devices can be considered for static

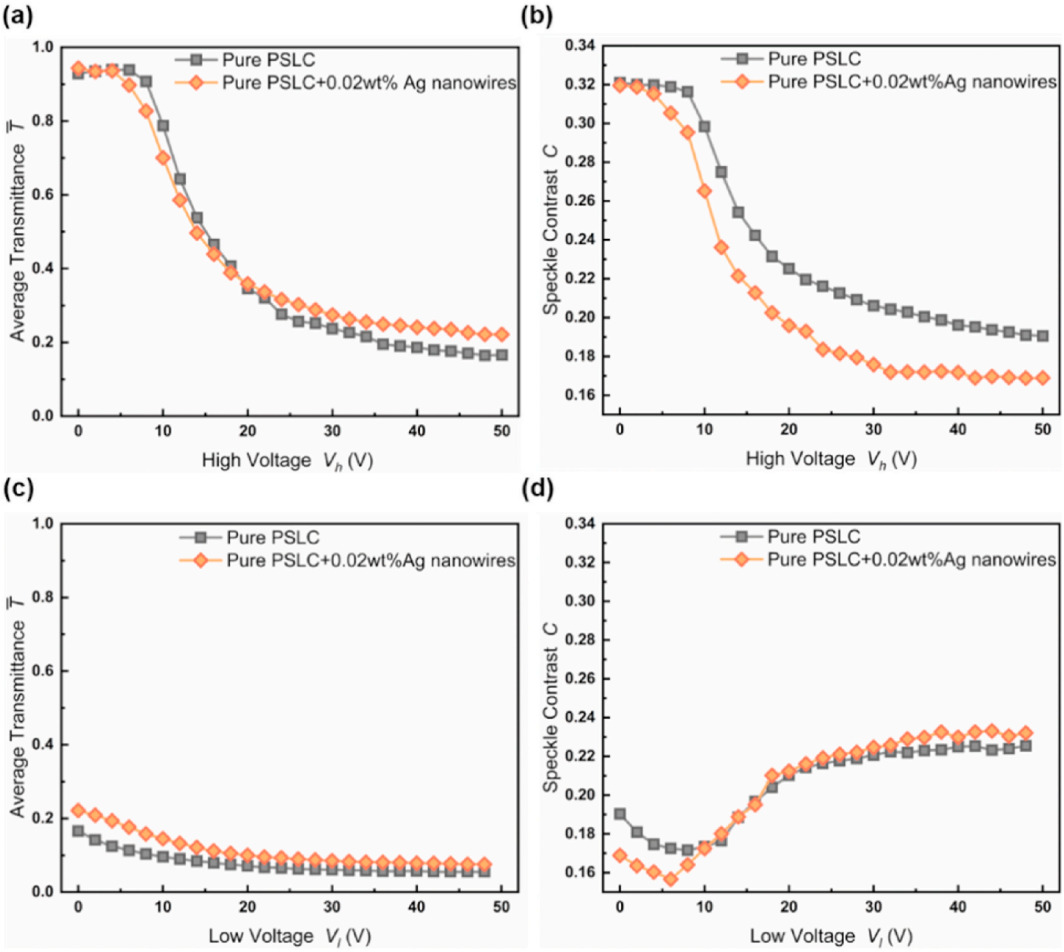

Fig. 10. Measured results for (a) high voltage–average transmittance (V_h–$\overline{T}$) curves and (c) low voltage–average transmittance (V_l – $\overline{T}$) curves, and (b) dependence of the speckle contrast (C) on the variable high voltage (V_h) and (d) on the variable low voltage (V_l) for both pure PSLC and PSLC doped with Ag nanowires.

modulation. The lower the value of $\overline{T}$, the higher the degree of decoherence. The best speckle-reduction effect was achieved when V_l was set to 8 V for sample A1. The speckle contrast C was reduced from 0.32 to 0.17, and the speckle-reduction efficiency was 46.9 %. Thus, to obtain optimal speckle reduction, we can set the optimal low-voltage V_l as the threshold voltage V_{th} of the PSLC devices.

4.2. *Effect of response time of PSLC doped with Ag nanowires on speckle contrast*

To obtain a higher speckle-reduction efficiency and better electro-optical properties, 0.02 wt% of Ag nanowires were doped into a pure PSLC. The optimal polymer concentration of the PSLC was chosen as 3 wt%. The high and low voltages were varied separately to determine the optimal square-wave AC signal driven at 25 Hz. The measured V-$\overline{T}$ and V–C curves for the pure PSLC and PSLC doped with Ag nanowires are shown in Fig. 10.

From Fig. 10(a) and (b), we can see that $\overline{T}$ of both pure PSLC and PSLC doped with Ag nanowires decrease with an increase in V_h. However, the PSLC doped with Ag nanowires had a lower V_{th} and V_{sat}, which is beneficial for reducing the driving voltage of PSLC devices. When $V_{th} = 9$ V was required for a pure PLSC device, $V_{th} = 6$ V was enough for a PSLC doped with Ag nanowires, which is 33.3 % lower. Similarly, when $V_{sat} = 32$ V was required for the pure PSLC device, $V_{sat} = 24$ V was enough for the PSLC doped with Ag nanowires, which was reduced by 25 %. For $V_h < 18$ V, $\overline{T}$ of the PSLC doped with Ag nanowires decreased faster than that of the pure PSLC; for $V_h > 18$V, the pure PSLC had a lower $\overline{T}$. Similar excellent electro-optical properties have also been reported for nematic LCs doped with metal nanomaterials [33,34]. The doping of Ag nanowires changes the electric flux path that is gathered around the Ag nanowires. Along with the increase in the electric flux density around the Ag nanowires, the electric field strength increases accordingly. As a result, LC molecules can be driven at a lower V_h, and in turn, lower V_{th} and V_{sat} as well as faster rates of transmittance variation, can be achieved. After saturation is reached for both pure PSLC and PSLC doped with Ag nanowires, $\overline{T}$ is influenced only by the polymer network. Theoretically, a lower $\overline{T}$ corresponds to lower speckle contrast. The speckle-reduction efficiency of PSLC doped with Ag nanowires was significantly better than that of the pure PSLC as shown in Fig. 10(b), which is mainly affected by the response time of the PSLC devices.

The relationships between $\overline{T}$ and C for different V_l values are shown in Fig. 10(c) and (d). As V_l increased, $\overline{T}$ for both pure PSLC and PSLC doped with Ag nanowires continuously decreased and tended to saturate. When $V_l < V_{th}$, C of the PSLC devices continuously decrease, and when $V_l = V_{th}$, optimal speckle-reduction efficiency is achieved. When $V_l > V_{th}$, the speckle contrast for both continues to increase until saturation. In the saturated state, both $\overline{T}$ and C of the PSLC doped with Ag nanowires were higher than those of the pure PSLC, and the mechanism is consistent with that in Section 4.1, when changing V_l. The lower $\overline{T}$ of the PSLC in saturation (considered as static modulation), the higher the degree of decoherence, which corresponds to a lower C. Thus, doping Ag nanowires into an LC mixture improves the electro-optical properties and speckle-reduction efficiency of PSLC devices.

Note that at saturation, $\overline{T}$ of the PSLC doped with Ag nanowires was not lower than that of the pure PSLC, which seems unfavorable for speckle reduction. The difference in $\overline{T}$ between the pure PSLC and PSLC doped with Ag nanowires is small because $\overline{T}$ is mainly determined by the polymer concentration. To confirm the reason why Ag nanowires improve the efficiency of speckle reduction, response time was measured using the experimental setup shown in Fig. 4 for both pure PSLC and PSLC doped with Ag nanowires. When the optimal modulation voltages were applied and the driving signal was set to a 25 Hz square wave, the response times of samples A1 and B1 were measured, as shown in Fig. 11(a). There was a small difference in t_{off} between sample B1 (6.2 ms) and sample A1 (6 ms), because the turn-off process mainly depends on the elastic response of the polymer network. Additionally, the LC molecules were reoriented by the vertically oriented layer and polymer network after removing V_h. The difference in t_{off} between the two samples can be reduced by optimizing the modulation square-wave AC signal, and the Ag nanowires have little effect on it. However, t_{on} of the

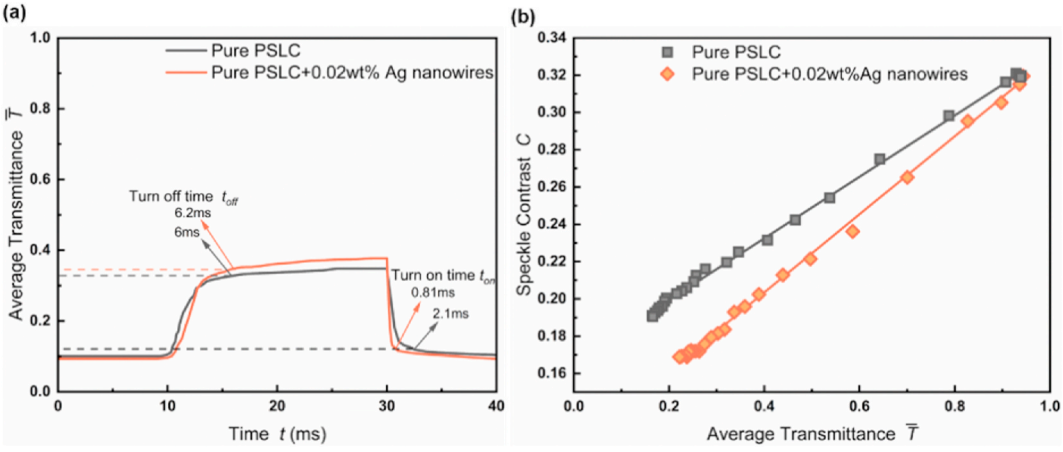

Fig. 11. Measured results of response time for both PSLC doped with Ag nanowires and pure PSLC: (a) comparison of response time for pure PSLC and 0.02 wt% Ag nanowires doped PSLC; (b) relationship between the speckle contrast and the response time with $\overline{T}$ for both PSLC doped with Ag nanowires and pure PSLC.

PSLC doped with Ag nanowires was only 0.81 ms, which was 61.4 % lower than that of the pure PSLC. This is because the turn-on process of the PSLC devices is mainly affected by the dielectric response, and Ag nanowire doping can effectively reduce the ionic impurities in LC and enhance the electric field strength, thus improving the dielectric response. Moreover, Ag nanowire doping can increase the polarity anchoring energy in PSLC, which would also shorten t_{on} [30].

Fig. 11(b) shows the relationship between $\overline{T}$ and C for both PSLC doped with Ag nanowires and pure PSLC. The value of C decreases significantly as the transmittance decreases, and the relationship between C and $\overline{T}$ is almost linear. This phenomenon also confirms that a reduction in $\overline{T}$ is favorable for suppressing C. Simultaneously, when the driving voltage was less than V_{th} or higher than V_{sat}, the decrease in $\overline{T}$ had no significant effect on C. Therefore, most measured data were gathered at both ends of the fitting curve. Most importantly, the PSLC doped with Ag nanowires exhibited a higher speckle-reduction efficiency than that of the pure PSLC at the same transmittance, and this phenomenon became increasingly obvious as the transmittance decreased. Therefore, the fitting curve for the PSLC doped with Ag nanowires was lower than that of the pure PSLC, as shown in Fig. 11(b), which is caused by the reduction in response time. A faster response time implies that more incoherent speckle patterns are involved in the superposition within the integration time. If LC molecules cannot be completely reoriented within the integration time, less incoherent speckle patterns are produced by the PSLC devices, and the speckle-reduction efficiency decreases. Therefore, the doping of Ag nanowires can significantly reduce the response time of PSLC devices, which is beneficial for further reducing speckle contrast.

A high degree of coherence is accompanied by unexpected background speckles across the overall image, causing severe information loss in imaging [35]. Coherence in the spatial domain can be reduced by dynamic scattering of PSLC devices under driving voltages, because dynamic scattering causes random time-varying amplitudes and phases at any point on the image plane. The decorrelation of the speckle patterns is better for higher scattering degrees. Therefore, the phase fluctuation of the light field in space is smaller, which results in better speckle reduction. In our experiments, the variation in the degree of scattering was controlled by changing the modulation voltage and polymer concentration. In addition, speckle patterns in the spatial domain can be averaged within the exposure time of the CMOS camera. Therefore, the faster response time of PSLC devices indicates that more decorrelated speckle patterns are superimposed over a specific period. In this study, the response time of PSLC devices was effectively improved by doping with Ag nanowires, and it was demonstrated that the response time is beneficial for improving speckle reduction.

4.3. Speckle reduction under the optimized driving condition of PSLC devices

Fig. 12 shows the speckle patterns and the variation of their grayscale value with pixel distance, which were generated after the laser light passed through the PSLC doped with 0.02 wt% Ag nanowires without driving voltage and with the optimized driving condition ($f = 25$ Hz, $V_l = 6$ V, $V_h = 50$ V). When the PSLC doped with Ag nanowires is in the “off” state (without driving voltage), the image shows a strong speckle with $C_0 = 0.321$; when the PSLC doped with Ag nanowires is in the “on” state with optimal modulation voltages, the image shows a weaker speckle with $C = 0.156$, which corresponds to a speckle-reduction efficiency of 51.4 %. Fig. 12(a) and (b) show the recorded light spot and the variation of their grayscale value with pixel distance, respectively, when the PSLC device is without a driving voltage, which corresponds to the situation of no PSLC device, whereas Fig. 12(c) and (d) show those obtained using a PSLC doped with Ag nanowires for speckle reduction. The fluctuations in Fig. 12(d) are significantly smaller than that in Fig. 12 (b), indicating that the laser speckle was significantly reduced by the developed PSLC device doped with Ag nanowires.

This performance indicates that doping with Ag nanowires is feasible. As shown in Fig. 10(d), the PSLC doped with Ag nanowires can further improve the speckle-reduction efficiency (46.9 %) compared to the pure PSLC. This method is a simple way to prepare PSLC and can achieve the same or even better speckle-reduction efficiency than other methods at low driving voltages. Moreover, its small size and static characteristics make it suitable for application in many speckle-reduction scenarios.

5. Conclusions

In this study, we demonstrate the excellent electro-optical properties and speckle reduction of PSLC devices doped with Ag nanowires. The doping of Ag nanowires effectively reduces the ionic impurities in LCs and, in turn, increases their dielectric response, which facilitates the superposition of more speckle patterns within the integration time. The effects of scattering degree and response time on speckle reduction were demonstrated by varying the polymer concentration, optimizing the driving voltage, and doping Ag nanowires. A PSLC device doped with 0.02 wt% Ag nanowires and 3 wt% polymer was demonstrated to achieve the most effective speckle reduction in the experiments. Under these optimized conditions, the threshold ($V_{th} = 6$ V) and saturation ($V_{sat} = 24$ V) voltages were decreased by 33.3 % and 25 %, respectively. The speckle contrast decreased from the initial value of $C_0 = 0.321$ to $C = 0.156$ for the developed PSLC device, and the speckle-reduction efficiency was 51.4 %. Moreover, the developed PSLC doped with Ag nanowires has the advantages of miniaturization, pure static, low driving voltage, and a simple fabrication process; therefore, it has good prospects for applications in laser imaging. However, the inclusion of PSLC in the optical path unavoidably causes a loss of light intensity, while the speckle contrast C still could not meet human-eye sensitivity (lower than 5 %). In future studies, we plan to reduce the loss of light intensity and speckle contrast by further optimizing the composition of the PSLC and doping material or by combining the developed PSLC devices with other static optical elements.

Funding

This work was supported by the National Natural Science Foundation of China (61975183) and the National Key R&D Program of

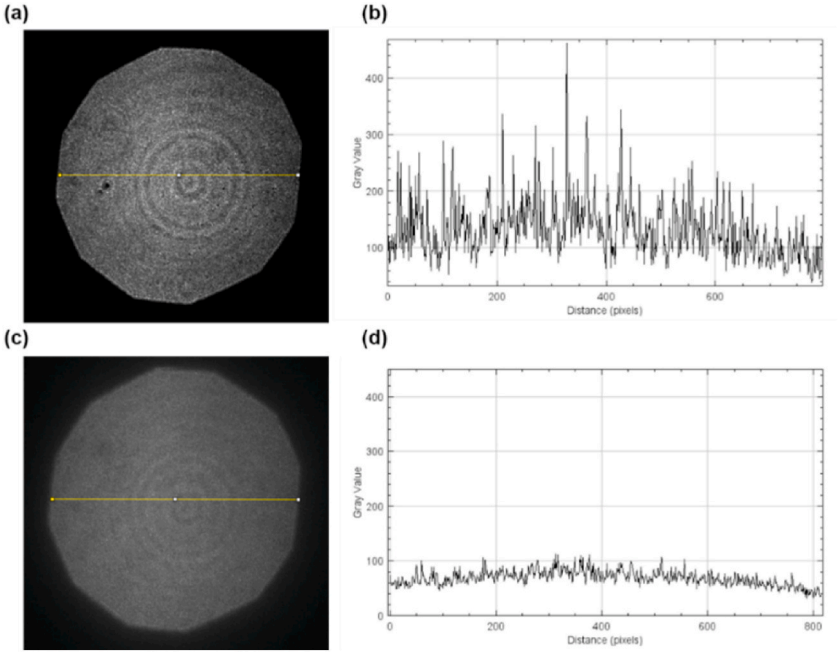

Fig. 12. Speckle patterns and their grayscale images: (a) light spot without PSLC device ($C_0 = 0.321$); (b) grayscale value with pixel distance for the yellow line in (a); (c) light spot with a PSLC doped with 0.02 wt% Ag nanowires and driven by optimal voltages ($C = 0.156$); (d) grayscale value with pixel distance for the yellow line in (c).

China (2018YFB0504603).

Data availability statement

The data underlying the results presented in this paper are not publicly available at this time but may be obtained from the authors on request.

CRediT authorship contribution statement

Xin Jiang: Writing – original draft, Visualization, Validation, Methodology, Investigation, Formal analysis, Data curation, Conceptualization. **Weilong Zhou:** Visualization, Validation, Investigation, Formal analysis, Data curation. **Wei Wang:** Visualization, Formal analysis. **Zichun Le:** Writing – review & editing, Writing – original draft, Validation, Supervision, Resources, Project administration, Methodology, Investigation, Funding acquisition, Conceptualization. **Wen Dong:** Visualization, Resources, Investigation, Formal analysis, Data curation.

Declaration of competing interest

The authors declare that they have no known competing financial interests or personal relationships that could have appeared to influence the work reported in this paper.

References

[1] K.V. Chellappan, E. Erden, H. Urey, Laser-based displays: a review, Appl. Opt. 49 (25) (2010) F79–F98.
[2] H. Zuo, S. He, FPCB micromirror-based laser projection availability indicator, IEEE Trans. Ind. Electron. 63 (5) (2016) 3009–3018.
[3] Y. Hou, Z. Zhou, C. Zhang, J. Tang, Y. Fan, F.-F. Xu, Y.S. Zhao, Full-color flexible laser displays based on random laser arrays, Sci. China Mater. 64 (11) (2021) 2805–2812.
[4] Y. Guo, J. Deng, J. Li, J. Zhou, D. Cai, Z. Le, Static laser speckle suppression using liquid light guides, Opt Express 29 (9) (2021) 14135–14150.
[5] J.W. Goodman, Speckle Phenomena in Optics: Theory and Applications, Ben Roberts and Company, 2007.
[6] B. Redding, M.A. Choma, H. Cao, Speckle-free laser imaging using random laser illumination (vol 6, p. 355, 2012)," Nat. Photonics 6 (7) (2012) 497, 497.
[7] A.S. Lapchuk, Q. Xu, Z. Le, J. Zhou, Z. Liu, D. Cai, O.V. Prygun, A.A. Kryuchyn, Theory of speckle suppression in a laser projector based on a long multimode fiber, Opt Laser. Technol. 144 (2021), https://doi.org/10.1016/j.optlastec.2021.107416.
[8] B. Redding, G. Allen, E.R. Dufresne, H. Cao, Low-loss high-speed speckle reduction using a colloidal dispersion, Appl. Opt. 52 (6) (2013) 1168–1172.
[9] K. Shigeo, W. Joseph, J. Goodman, Very efficient speckle contrast reduction realized by moving diffuser device, Appl. Opt. 49 (23) (2010).
[10] J. Xue, Z. Tong, Y. Ma, M. Wang, S. Jia, X. Chen, Fabrication of volume scattering diffusers by spin-coating SiO2 microspheres and SU-8 photoresist for speckle reduction investigation, Opt. Mater. Express 12 (2) (2022).
[11] J. Li, Design of optical engine for LCOS laser display with rotated diffuser plate, Microw. Opt. Technol. Lett. 55 (1) (2013) 138–141.

[12] S. Mahler, Y. Eliezer, H. Yılmaz, A.A. Friesem, N. Davidson, H. Cao, Fast laser speckle suppression with an intracavity diffuser, Nanophoton 10 (1) (2021) 129–136.
[13] D.S. Mehta, D.N. Naik, R.K. Singh, M. Takeda, Laser speckle reduction by multimode optical fiber bundle with combined temporal, spatial, and angular diversity, Appl. Opt. 51 (12) (2012) 1894–1904.
[14] M.N. Akram, Z. Tong, G. Ouyang, X. Chen, V. Kartashov, Laser speckle reduction due to spatial and angular diversity introduced by fast scanning micromirror, Appl. Opt. 49 (17) (2010) 3297–3304.
[15] Z. Le, Z. Liu, Y. Qiu, H. Ren, Y. Dai, Fabrication of ultrathin flexible diffractive optical elements (DOEs) and application for laser speckle suppression, Opt. Lasers Eng. 159 (2022), https://doi.org/10.1016/j.optlaseng.2022.107223.
[16] Z. Le, A. Lapchuk, I. Gorbov, Z. Lu, S. Yao, I. Kosyak, T. Kliuieva, Y. Guo, O. Prygun, Theory and experiments based on tracked moving flexible DOE loops for speckle suppression in compact laser projection, Opt. Lasers Eng. 124 (2020), https://doi.org/10.1016/j.optlaseng.2019.105845.
[17] A. Lapchuk, O. Prygun, M. Fu, Z. Le, Q. Xiong, A. Kryuchyn, Dispersion of speckle suppression efficiency for binary DOE structures: spectral domain and coherent matrix approaches, Opt Express 25 (13) (2017) 14575–14597.
[18] V. Kumar, K. Usmani, V. Singh, A.K. Dubey, M. Gupta, D.S. Mehta, Laser speckle reduction using spatially structured and temporally varying beams using double diffractive optical elements, Laser Phys. Lett. 17 (3) (2020), 036003.
[19] I. Kompanets, N. Zalyapin, Methods and devices of speckle-noise suppression (review)," Opt. Photonics J. 10 (10) (2020) 219–250.
[20] Z. Tong, Q. Gao, Y. Yan, Y. Ma, M. Wang, S. Jia, X. Chen, Electroactive despeckle diffuser using polymer dispersed liquid crystal in-plane switched by interdigitated electrodes, Opt Laser. Technol. 145 (2022), 107541, https://doi.org/10.1016/j.optlastec.2021.107541.
[21] H. Ishikawa, A. Shibase, W. Weng, M. Ono, H. Furue, Reduction of laser speckle noise by using particle-dispersed liquid crystals, Mol. Cryst. Liq. Cryst. 646 (1) (2017) 93–98.
[22] H. Furue, Y. Sugimoto, K. Iwami, W. Weng, M. Ono, Control of laser speckle noise by using polymer-dispersed LC, Mol. Cryst. Liq. Cryst. 612 (1) (2015) 245–250.
[23] H. Furue, A. Terashima, M. Shirao, Y. Koizumi, M. Ono, Control of laser speckle noise using liquid crystals, Jpn. J. Appl. Phys. 50 (9) (2011) 1489–1496.
[24] D.J. Hansford, J.A.J. Fells, S.J. Elston, S.M. Morris, Speckle contrast reduction of laser light using a chiral nematic liquid crystal diffuser, Appl. Phys. Lett. 109 (26) (2016), 261104.
[25] J.H. Lin, S.C. Chang, Y.H. Li, C.Y. Chien, C.H. Chen, Y.C. Lin, J.J. Wu, S.Y. Tsay, Y.H. Chen, Investigation of laser speckle noise suppression by using polymer-stabilized liquid crystals within twisted nematic cell, Appl. Phys. Express 10 (3) (2017), 031701.
[26] D.J. Hansford, Y. Jin, S.J. Elston, S.M. Morris, Enhancing laser speckle reduction by decreasing the pitch of a chiral nematic liquid crystal diffuser, Sci. Rep. 11 (1) (2021) 4818.
[27] Y.H. Chen, J.W. Pan, S.C. Jeng, A low speckle laser pico-projector using dynamic light scattering liquid crystal devices, Displays 75 (2022), https://doi.org/10.1016/j.displa.2022.102305.
[28] A.L. Andreev, T.B. Andreeva, I.N. Kompanets, N.V. Zalyapin, Space-inhomogeneous phase modulation of laser radiation in an electro-optical ferroelectric liquid crystal cell for suppressing speckle noise, Appl. Opt. 57 (6) (2018) 1331–1337.
[29] J.H. Lin, K.C. Liao, L.H. Jian, S.Y. Tsay, J.-J. Wu, Y.-G. Duann, Spatially tunable emissions of dye-doped liquid crystal lasers between the cholesteric and smectic phases, Opt. Mater. Express 5 (10) (2015) 2142–2149.
[30] X. Yan, W. Liu, Y. Zhou, D. Yuan, X. Hu, W. Zhao, G. Zhou, Improvement of electro-optical properties of PSLC devices by silver nanowire doping, Appl. Sci. Basel 9 (1) (2019) 145.
[31] Y. Jin, N.P. Spiller, C. He, G. Faulkner, M.J. Booth, S.J. Elston, S.M. Morris, Zwitterion-doped liquid crystal speckle reducers for immersive displays and vectorial imaging, Light Sci. Appl. 12 (2023) 242, https://doi.org/10.1038/s41377-023-01265-5.
[32] D.J. Hansford, A Liquid Crystal Device for Speckle Reduction in Coherent Light, University of Oxford, Oxford, 2018.
[33] C.H. Chan, T.Y. Wu, M.H. Yen, C.E. Lin, K.T. Cheng, C.C. Chen, Low power consumption and high-contrast light scattering based on polymer-dispersed liquid crystals doped with silver-coated polystyrene microspheres, Opt Express 24 (26) (2016) 29963–29971.
[34] H.M. Lee, H.K. Chung, H.G. Park, H.C. Jeong, J.J. Han, M.J. Cho, J.W. Lee, D.S. Seo, Residual DC voltage-free behaviour of liquid crystal system with nickel nanoparticle dispersion, Liq. Cryst. 41 (2) (2014) 247–251.
[35] H. Farrokhi, T.M. Rohith, J. Boonruangkan, S. Han, H. Kim, S.W. Kim, Y.J. Kim, High-brightness laser imaging with tunable speckle reduction enabled by electroactive micro-optic diffusers, Sci. Rep. 7 (1) (2017), 15318.